Laboratori Nazionali di Frascati

LNF–10/ 12 (IR)
March 31, 2010

SPECTRAL CHARACTERISTICS OF PLANAR CHANNELING RADIATION BY 20-800 MEV ELECTRONS IN A THIN SILICON CARBIDE

B. Azadegan[a], and S.B. Dabagov[b,c]

[a] *Sabzevar Tarbiat Moallem University, Sabzevar, Iran*
[b] *INFN Laboratori Nazionali di Frascati, Via E. Fermi 40, 00044 Frascati (RM), Italy*
[c] *RAS P.N. Lebedev Physical Institute, Leninsky Pr. 53, 119991 Moscow, Russia*

Abstract

Spectral distributions of channeling radiation by 20÷800 MeV electrons in different planes of a thin 4H polytype silicon carbide crystal is presented. We demonstrated that channeling in 4H SiC with hexagonal structure has some new features not available in other structures. Using Doyle-Turner approximation to the atomic scattering factor and taking in to account thermal vibrations of atoms, the continuum potentials for different planes of 4H polytype SiC single crystal were calculated. In the frame of quantum mechanic, the theory of channeling radiation has been applied to calculate the transverse electron states in the continuum potential of the planes and to study transition energies, linewidths, depth dependence for population of quantum states and spectral radiation distributions. At electron energies higher than 100 MeV the spectral distributions of radiation are calculated by classical calculations and successfully compared with quantum mechanics solutions. Specific properties of planar channeling radiation in 4H polytype SiC are discussed.

PACS.: 61.85.+p

Published by
Servizio Informazione e Documentazione Scientifica dei LNF
Ufficio Biblioteca e Pubblicazioni

1 – INTRODUCTION

Channeling radiation is emitted by relativistic charged particles during passing through a single crystal near parallel to some axes or planes. Channeling radiation emitted by electrons has mainly been studied on monatomic crystals such as diamond [1-3], Si [4-6], Ge [7-8], and on metals (e.g. Be, Ni, Sb, W [9-11]). Binary or polyatomic crystals (e.g. LiH [12], LiF [13-14], GaAs, ruby [15]) have scarcely been utilized. Most of the above mentioned crystals are characterized by a cubic lattice. In such crystals, intense CR is observed from the planes with low crystallographic indices such as (100), (110) and (111). In our previous papers [16-17] we investigated CR from different planes of quartz crystal (SiO_2), which has a hexagonal structure. The more complicate crystal structure of the binary quartz crystal (compared with cubic crystals such as, e.g., diamond, Si or Ge) allows channeling for planes with relatively large indices, which have rather deep potentials and out of which CR can be observed. Therefore, we may observe some specific properties of channeling radiation in other types of crystals with hexagonal structure such as SiC.

The aim of the paper is to comment on the validity of both quantum mechanical and classical approaches for the theory of channeling radiation (CR) by relativistic electrons in thin SiC crystal.

2 – THEORY

2.1 – Crystal

A 4H-SiC crystal is characterized by a hexagonal structure containing 4 Si and 4 O atoms in the unit cell as shown in Fig. 1. This is a hexagonal lattice, belonging to the space group $P6_3mc$ and each Si ion is surrounded by a tetrahedra of C ion, and vice-versa. The 4H refers to the fact that there are 4 SiC dimmers in the hexagonal unit cell. Its lattice is defined by two primitive vectors **a**, **b** of equal length, which make an angle of 120° with each other, and a third one **c** is perpendicular to both the others. The primitive vectors in the Cartesian coordinates system are

$$\vec{a}_1 = a(\frac{1}{2}\hat{x} - \frac{\sqrt{3}}{2}\hat{y}), \quad \vec{a}_2 = a(\frac{1}{2}\hat{x} + \frac{\sqrt{3}}{2}\hat{y}), \quad \vec{a}_3 = c\hat{z},$$

where in 4H-SiC a and c are 3.0805 and 10.0848 Å, respectively [22]. The primitive vectors for reciprocal lattice are

$$\vec{b}_1 = \frac{2\pi}{a}(\hat{x} - \frac{1}{\sqrt{3}}\hat{y}), \quad \vec{b}_2 = \frac{2\pi}{a}(\hat{x} + \frac{1}{\sqrt{3}}\hat{y}), \quad \vec{b}_3 = \frac{2\pi}{c}\hat{z}.$$

The coordinates of silicon and carbon atoms in the hexagonal coordinates system are

$$Si\ (I) : \{0, 0, Z_1 C\}, \{0, 0, (Z_1 + 1/2) C\}$$
$$C\ (I) : \{0, 0, Z_2 C\}, \{0, 0, (Z_2 + 1/2) C\}$$
$$Si\ (II) : \{1/2\, a, 1/\sqrt{12}\, a, Z_3 C\}, \{1/2\, a, -1/\sqrt{12}\, a, (Z_3 + 1/2) C\}$$
$$C\ (II) : \{1/2\, a, 1/\sqrt{12}\, a, Z_4 C\}, \{1/2\, a, -1/\sqrt{12}\, a, (Z_4 + 1/2) C\}$$

where in 4H-SiC Z_1=0.0, Z_2=0.1875, Z_3=0.249825, and Z_4=0.437325. In this form, a crystal plane is given by four indices (hkil) with i=-(h+k) where h, k, i and l are the Miller indices. The interplanar distance for a hexagonal structure is given by

$$\frac{1}{d_p^{\,2}} = \frac{4}{3}\left(\frac{h^2 + hk + k^2}{a^2}\right) + \frac{l^2}{c^2}.$$

The depth of potential well and the interplanar distance of the planes are very important in CR experiments which are depend on the Miller indices (hkil). Deeper potential wells have a larger number of the bound states, and larger interplanar distance produces lower initial population of the states. Therefore, in SiC crystal CR can be observed not only from the planes with low Miller indices but also from the planes with higher order of Miller indices.

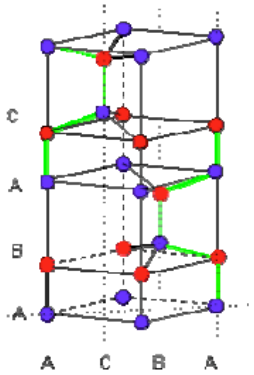

FIG. 1 – The hexagonal structure of SiC. Si atoms are shown as blue spheres, C atoms as red spheres. One unit cell is outlined for clarity.

B – Planar channeling radiation

At planar channeling the relativistic particle enters the crystal under a small incidence angle relative to the crystal plane considered. The description of planar CR bases on the division of the particle motion into both longitudinal and transverse components. Since, in first approximation the longitudinal motion along the plane of channeling is not affected by forces, the velocity in z direction is actually nearly constant $v_z \approx c$. However, under channeling condition, the transverse momentum p_x of the channeled particle is small compared to the longitudinal one p_z and, therefore, its transverse energy can be defined by the following expression

$$E_x = \frac{p_x^2}{2m\gamma} + V(x)\,, \tag{1}$$

with relativistic particle mass $m\gamma$ [18].

In order to describe the radiation emitted by the charged particle at channeling, the applicability of both classical and quantum theories have to be considered.

C – Continuum potential

Since the longitudinal component of relativistic electron velocity is near the speed of light, the crystal plane is assumed to be charged continuously (approximation of continuous potential [19]). Since the potential has the periodicity of the lattice, its expansion to a Fourier series represents the most general form of the continuum potential. The continuum potential expanded into a Fourier series reads

$$V(x) = \sum_n V_n e^{ingx}\,, \quad \text{n = …, -1, 0, 1, 2, ...} \quad , \tag{2}$$

where V_n denote the Fourier coefficients of periodic potential. Using the Doyle-Turner approach [21] for the electron-atom interaction the coefficients can be written as

$$V_n = -\frac{2\pi}{v_c} a_0^2 (e^2/a_0) \sum_j e^{-M_j(\vec{g})} e^{-i\vec{g}.\vec{r_j}} \sum_{i=1}^{4} a_i e^{\left(-\frac{1}{4}(\frac{b_i}{4\pi^2})(ng)^2\right)}\,, \tag{3}$$

where v_c is the volume of unit cell, a_0 is the Bohr radius, e is the electron charge, $\vec{r_j}$ represents the coordinates of the j atoms in the unit cell, a_i, b_i are the tabulated coefficients[21], and $M_j(\vec{g}) = \frac{1}{2} g^2 \left\langle u_j^2 \right\rangle$ denotes the Debye-Waller factor, which describes the thermal vibration of the j^{th} atom with mean squared amplitude $\langle u_j^2 \rangle$. The values of $\langle u^2 \rangle = 0.00666$ Å^2 for SiC were used as given in Ref. 22. Since the potential converge very fast, the sum over n can restrict to 21. The term $\sum e^{-i\vec{g}.\vec{r_j}}$ in Eq. (3) is the structure factor of a crystal. The structure factor determines those sets of Miller indices, (hkil), for which the reflections from the corresponding planes are strong. SiC belongs to the space group $P6_3m$ and the CR from planes with Miller indices l=0 will be observed. For such a crystal structure, the (hkil) and (khil) planes have equal interplanar distance and potential well. Calculated planar potential for electrons channeled along the $(11\bar{2}0)$ plane of SiC is shown in Fig. 2.

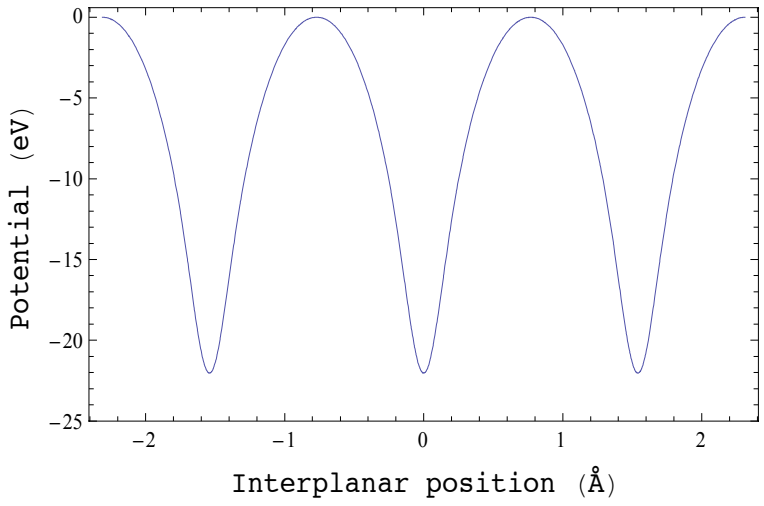

FIG. 2 – The $(11\bar{2}0)$ continuum potential for electrons.

D – Classical description of planar channeling radiation

Within the frame of the classical model, the scattering at the ordered crystal atoms becomes coherent now, causing an oscillatory motion of the electrons along the corresponding string or plane of atoms. Considering this oscillatory motion as an accelerated one in the rest frame of the electron, it emits electromagnetic radiation called channeling radiation (CR). Although the oscillation frequency ω_0 is rather low and corresponds to a radiation energy $\hbar\omega_0$ in the optical region, relativistic effects such as the Lorentz contraction of the longitudinal coordinate and the Doppler effect transform the energy of emitted CR photons observed in forward direction into the X-rays domain.

The equation of motion for relativistic particle in the one dimensional continuum potential $V(x)$ has the form

$$\gamma m \ddot{x}(t) = -\frac{\partial V(x)}{\partial x} \tag{4}$$

The initial conditions are: the point of incidence into the crystal $x(0) = x_0$ and the transverse momentum $p_x(0) = p\theta_0$ (θ_0 is the angle of incidence with respect to the crystallographic planes), which define the initial transverse energy (Eq. (1))

$$E_x = \frac{p^2\theta_0^2}{2\gamma m} + V(x_0) \tag{5}$$

The energy density radiated in a solid angle $d\Omega$ and a frequency interval $(\omega, \omega+d\omega)$ has the following form [18]

$$\frac{d^2E}{d\omega d\Omega} = \frac{e^2}{4\pi^2 c}\left|\int_0^\tau e^{i(\omega t - \vec{k}.\vec{r})}\,\frac{\vec{n}\times((\vec{n}-\vec{\beta})\times\dot{\vec{\beta}})}{(1-\vec{\beta}.\vec{n})^2}\,dt\right|^2 , \qquad (6)$$

where, $\vec{\beta} = \vec{r}(t)/c$ is the particle velocity, $\vec{r}(t) = \vec{v}_z t + \vec{x}(t)$ is its trajectory, $\vec{k} = \omega\vec{n}/c$ is the wave vector, $\vec{n}$ is the unit vector defining the direction of photon emission, e is the charge of electron and τ is penetration time of the particle through the crystal. Eq. (6) is the base for calculations of CR spectra in the frame of classical mechanic.

E – Quantum description of planar channeling radiation

In the frame of the quantum mechanical model, the transverse motion of the channeled electrons of mass $m\gamma$ can be described by a one (planar) dimensional Schrödinger equation, which contains the averaged potential of the crystal. The transverse motion of the channeled electrons is, therefore, restricted to discrete (bound) channeling states of so-called continuum potential. Spontaneous transitions between these eigenstates lead to the emission of CR, the energy spectrum of which is consequently characterized by a line structure of possible photon energies. Quantum CR theory for relatively low-energy electrons is based on a Bloch wave solution of the Schrödinger equation for incident particle passing through periodic potential of a plane. In the case of planar CR the periodic potential is one dimensional that reduces the problem to the solution of one dimensional Schrödinger equation [2]

$$-\frac{\hbar^2}{2m_e\gamma}\frac{d^2\psi(x)}{dx^2} + V(x)\psi(x) = E\psi(x) \qquad (7)$$

Since the crystal potential is periodic, the solutions of Eq. (7) are the Bloch waves [2]

$$\psi(x) = e^{ikx}\sum_n c_n e^{ingx}, \quad \text{n} = \ldots, -1, 0, 1, 2, \ldots , \qquad (8)$$

where k is the electron wave vector and $\vec{g}$ is the reciprocal lattice vector of the plane. Substitution of Eqs. (2) and (8) into Eq. (7) reduces the problem to calculating the eigenvalues of a matrix $\boldsymbol{A}$, which in the planar case consists of the following components:

$$\begin{aligned} A_{nm} &= V_{n-m} \qquad (n \neq m) \\ A_{nn} &= \frac{\hbar^2}{2m\gamma}(k+ng)^2 + V_0 \end{aligned} \qquad (9)$$

Since the potential as well as the eigenvalues converge very fast one can restrict the solution to the 21 Bloch functions that leads to a problem of 21×21 matrix. The

spontaneous transition of a channeled electron from higher to lower transverse state leads to the emission of a CR photon.

The spontaneous transition rate of planar CR per unit of solid angle, per unit of photon energy and per electron is given in [9]. For CR directed along the electron motion, we can write [3]

$$\frac{d^3N_{CR}(i\to f)}{d\Omega_\gamma dE_\gamma}=\frac{\alpha\lambda_c^2}{\pi\hbar c}\int dk\ E_k^0\left|\left\langle\psi_{kf}\left|d/dx\right|\psi_{ki}\right\rangle\right|^2\int_0^L dzP_{ki}(z)\frac{(\Gamma_k/2)}{(E_\gamma-E_k^0)^2+0.25\Gamma_k^2}, \quad (10)$$

where $\left\langle\psi_{kf}\left|d/dx\right|\psi_{ki}\right\rangle$ is the transition matrix element, and $P_{ki}(z)$ gives the occupation probability of the channeling state i as a function of initial population and crystal thickness, $E_k^0=2\gamma^2(\varepsilon_{ki}-\varepsilon_{kf})$ is the photon energy of the *i-f* transition, and Γ_k is the intrinsic linewidth. It should be underlined that in Eq. (10) the first integral refers to the integral over the Bloch momenta, and the second integral refers to one over the occupation of the state i over a chosen crystal thickness L. Both intrinsic line width and occupation probability of the state i are calculated according to [3] and [17], respectively.

F – Applicability of classical and quantum considerations to planar channeling radiation in SiC

The applicability of both classical and quantum mechanical calculations in channeling can be estimated on the base of the level number in a continuum potential [18]. In low-energy region (several MeV) the particle motion has quantum character, while band structure effects appear for the higher-lying levels and the line structure of the emission spectrum is clearly pronounced. The calculations and experiments for planar channeling in silicon and diamond crystals along the main crystallographic directions show that the number of bound states is relatively small at electron energies less than 100 MeV, and, therefore, the quantum mechanical approach for description of CR becomes necessary. With electron energy increase, the density of bound states also increases leading to the states overlapping, and the band structure effects are less important. This situation can be handled within classical mechanics calculations.

In [20] the validity of both classical and quantum descriptions for channeling radiation by relativistic electrons in a thin LiF crystal is discussed. The halite structure of LiF leads to the planes consisting of Li and F ions and the planes, which are formed by only one kind of ions. The continuum potential of planes consisting of two types of ions, however, has usually two dips of different strength formed by either one or other kind of

crystal atoms, respectively. Consequently, the CR spectrum can contain a mixture of CR lines originating from transverse transitions of channeled electrons between the states localized in the different potential wells. They have demonstrated that the complicated shape of periodic (111) planar potential of LiF allows the existence of a different number of discrete energy levels, quantum states, in the potential well formed by Li atoms. Moreover, the potential well consisting of only F atoms is rather deep to apply the classical method. With increasing electrons energy, the classical method becomes valid to describe CR from under-barrier electrons in a deeper potential well, while one should still apply the quantum method to calculate CR from electrons in shallower potential well. They mentioned that the quantum feature of a CR spectrum from relativistic electrons maintains its quantum characteristics up to 2 GeV electron energies.

3 – CALCULATIONS

3. 1 – The $(11\bar{2}0)$ plane

Calculated planar potentials for electrons channeled along the $(11\bar{2}0)$ plane of SiC with eigenvalues and Bloch bands for 20 MeV electrons are shown in Fig. 3. At this energy the particle motion has quantum character, four states are bound and three single CR lines can be observed in the spectrum. The variation of the initial populations of bound states with the incidence angle for 20 MeV electrons is shown in Fig. 4. The depth dependence for the occupation $P_{kn}(z)$ of bound and quasi-free states determined for δz = 0.02 μm at electron energy of 20 MeV is shown in Fig. 5 where 0.5 mrad incidence angle of electron beam and zero beam divergence have been assumed. At depth of about 2 μm, statistical equilibrium for the states occupation is reached.

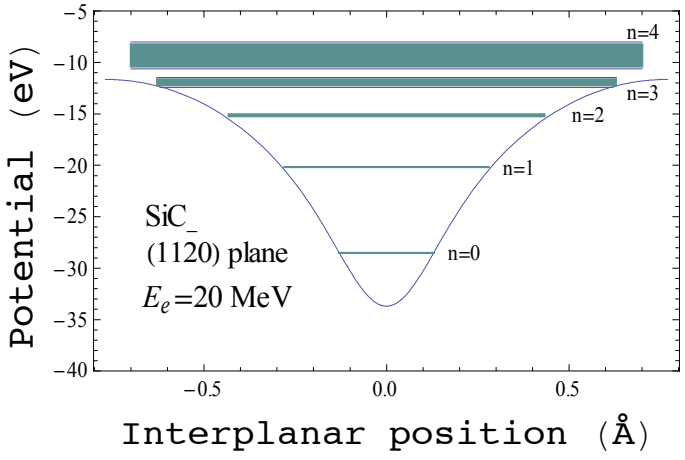

FIG. 3 – The $(11\bar{2}0)$ continuum potential and eigenvalues for 20 MeV electrons.

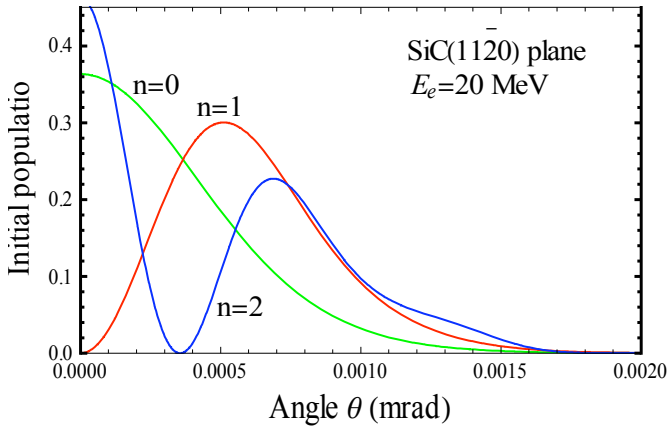

FIG. 4 – Initial populations of bound states in the (11$\bar{2}$0) plane of SiC drawn versus the incidence angle of 20 MeV electrons.

It is notable that only thermal scattering has been considered up to now. Although this is the main scattering process for thin crystals, at larger crystal thickness multiple scattering becomes also important. As shown above, equilibrium occupation is reached after a small penetration depth, but this does not mean that it holds over the entire crystal thickness. Channeled particles can be dechanneled, i.e., they will be scattered into the continuum leaving the channeling regime. Andersen et al. [5] already mentioned that for electrons of MeV energies the statistical equilibrium between channeling states and free states is quickly established. The depth dependence of the occupation of the low number of channeling states then may be obtained from random multiple scattering only, since a major fraction of beam particles populates the states in the continuum where electron scattering dominates. At fixed crystal thickness, the total CR photon yield can be obtained by integration of the occupation function over the entire crystal thickness. For illustration, CR spectra calculated by means of Eq. (10) for channeling in the (11$\bar{2}$0) plane of a 5 μm thick SiC crystal are shown in Fig. 6.

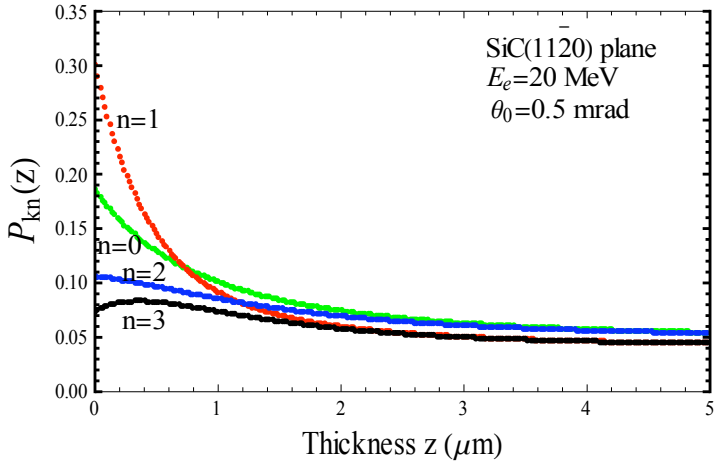

FIG. 5 – Depth dependence of the states occupation drawn versus the crystal thickness for 20 MeV electrons at 0.5 mrad incidence angle.

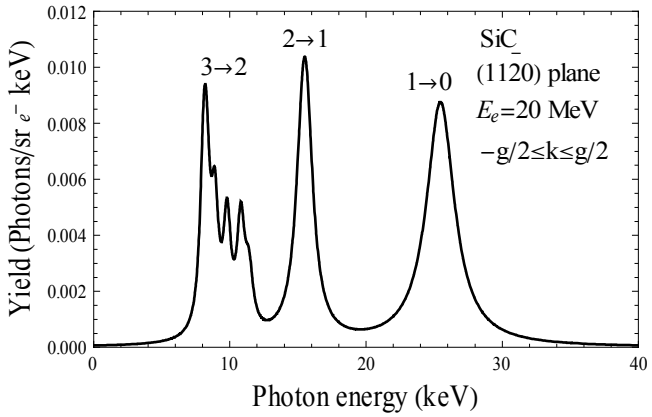

FIG. 6 – Simulation of the CR spectrum from 20 mev electrons channeled in the $(11\bar{2}0)$ plane of a 5 μm SiC crystal.

Fig. 7 shows the continuum potential along with eigenvalues and Bloch bands for 200 MeV electrons channeled along the $(11\bar{2}0)$ plane of SiC. At this energy 10 states are bound and it seems that channeling has classical character. In order to calculate the spectral angular distribution of CR for electrons of energies 200 MeV , we substituted into Eq. (6) the trajectories, velocities and acceleration of electrons obtained by numerical solution of the equation of motion (4) in the $(11\bar{2}0)$ potential of SiC calculated by means of equations (2) and (3). Fig. 8 shows a typical CR spectra emitted in the forward direction by 200 MeV energy electron penetrating into a 10 μm thick SiC crystal at chosen incidence angle and point.

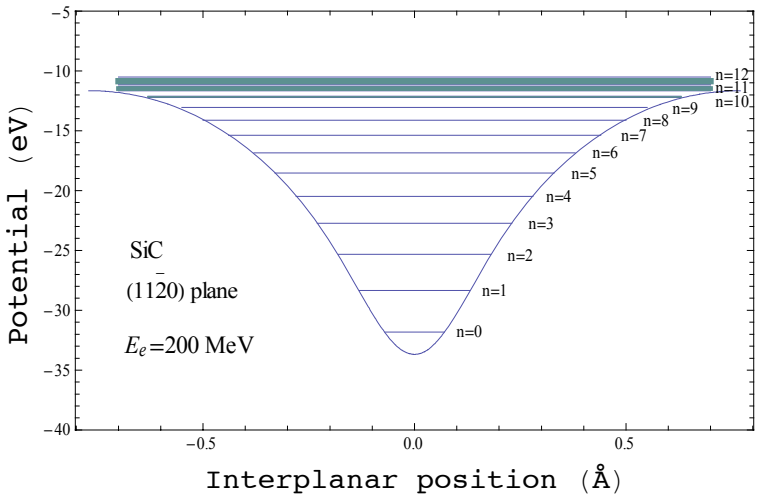

FIG. 7 – The $(11\bar{2}0)$ continuum potential and eigenvalues for 200 MeV electrons.

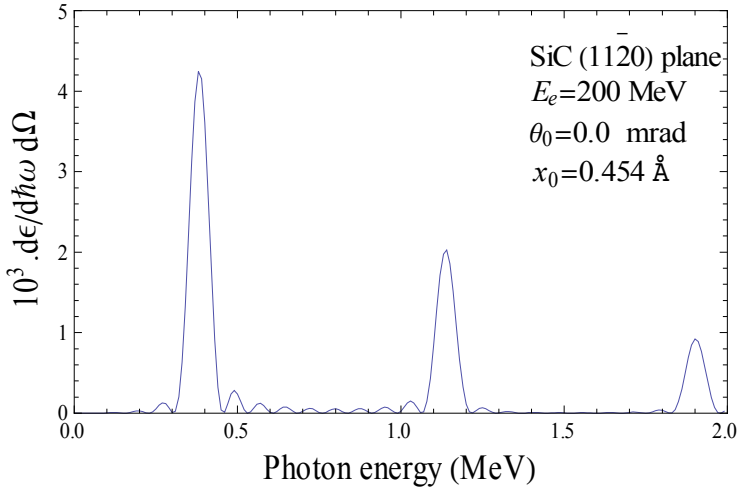

FIG. 8 – Spectral angular distribution of forward emitted photons by 800 MeV electrons trapped by (11$\bar{2}$0) plane of 10 μm thick SiC crystal.

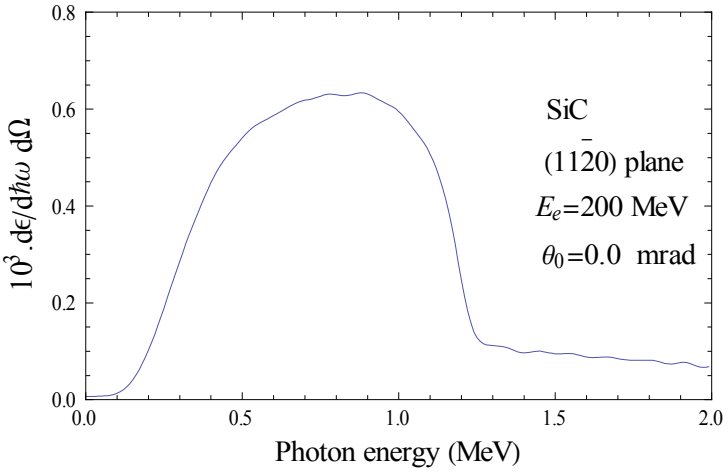

FIG. 9 – Spectral angular distribution of CR averaged over points of incidence from 200 MeV electrons trapped by the (11$\bar{2}$0) plane of a 5 μm thick SiC crystal.

In practice, a beam of electrons hints a crystal surface forming different initial conditions for various electrons. Therefore, one has to find the spectral distribution of radiation for all points of incidence (possible trajectories). The total observed spectra obtains by averaging over partial spectral distributions. Fig. 9 shows the averaged spectral angular distribution of CR emitted in the forward direction by 200 MeV electrons in a 10 μm thick SiC crystal. In this intermediate energy region, however, for some specific cases CR is described with the same accuracy by both classical and quantum methods. In order to compare the classical calculations with quantum ones the spectral angular distribution of CR for 200 MeV energy electrons is simulated by a quantum method (Fig. 10). As seen, the energy distributions of both spectra (Figs. 9 and 10) are nearly the same but line structure is still seen for quantum approximation. In quantum mechanical model if one can assume that higher states have a shorter coherence lifetime and, therefore, bigger linewidth then classical and quantum methods give the same results.

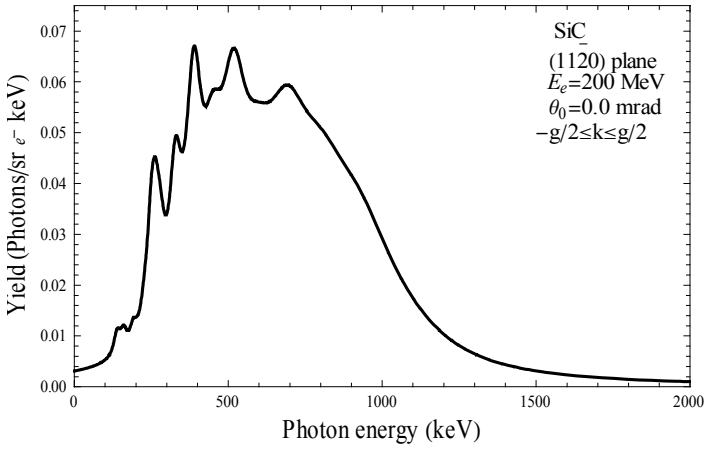

FIG. 10 – Quantum simulation of the CR spectrum for channeling of 200 MeV electrons in the (11$\bar{2}$0) plane of a 5 μm thick SiC crystal.

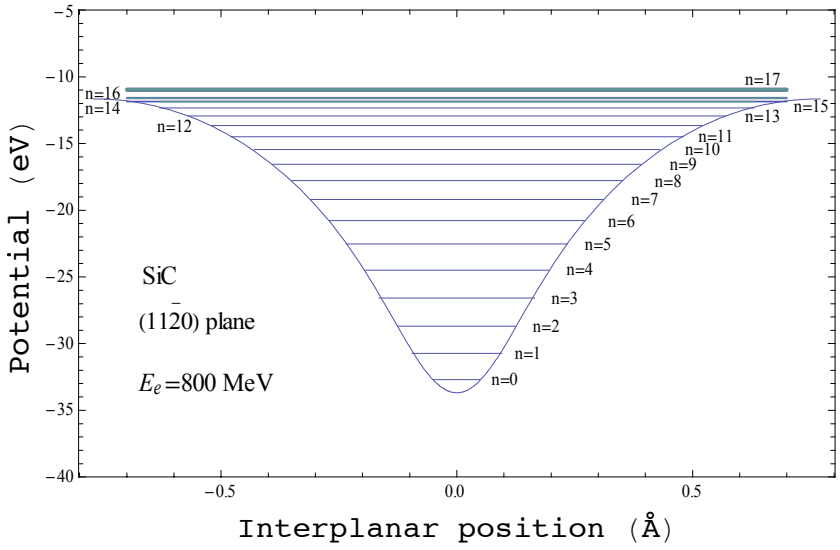

FIG. 11 – The (11$\bar{2}$0) continuum potential and eigenvalues for 800 MeV electrons.

The number of bound states increases from four to ten with increasing the electron energy from 20 MeV to 200 MeV. For electron channeling radiation in SiC the transition from line emission to unstructured "humps" can be observed. With increasing the electrons energy from 200 MeV to 800 MeV the number of bound states changes from 10 to 14 (Figs. 7 and 11). At electron energy of 800 MeV, it seems, classical method can be applied successfully. Fig. 12 shows the spectral angular distribution of CR for electrons of energy 800 MeV that is simulated within the classical approach.

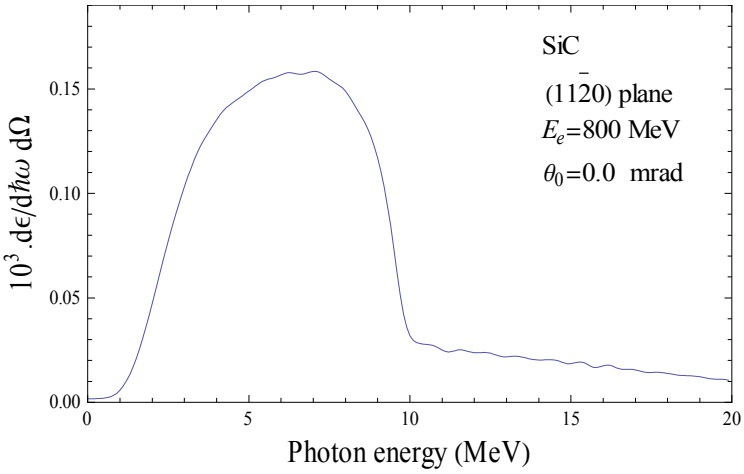

FIG. 12 – Spectral angular distribution of CR averaged over points of incidence from 800 MeV electrons channeled in the $(11\bar{2}0)$ plane of a 10 μm thick SiC crystal.

3. 2 – The $(21\bar{3}0)$ plane

The $(21\bar{3}0)$ plane of SiC has a rather shallow potential (Fig. 13). At electron energy of 100 MeV, only two states with $n = 0$ and $n = 1$ are bound. Therefore, only one CR line corresponding to the transition 1→0 can be observed (Fig.15).

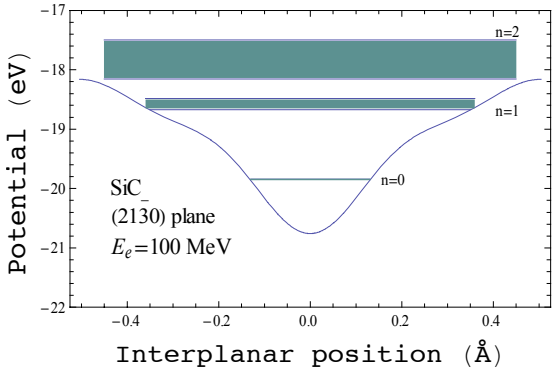

FIG. 13 – The $(21\bar{3}0)$ continuum potential and eigenvalues for 100 MeV electrons.

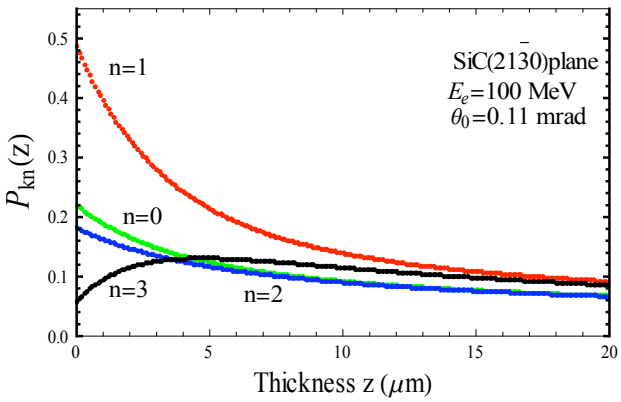

FIG. 14 – Depth dependence of the states occupation versus the crystal thickness for 100 MeV electrons at 0.11 mrad incidence angle.

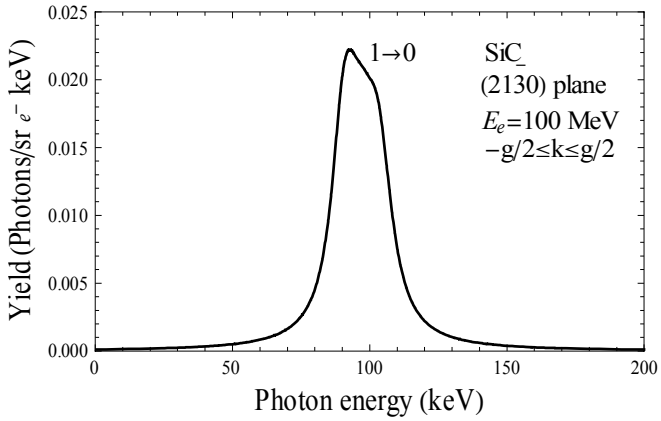

FIG. 15 – Simulation of the CR spectrum for channeling of 100 MeV electrons in the $(21\bar{3}0)$ plane of a 20 μm thick SiC crystal.

3. 3 – The $(41\bar{5}0)$ plane

The $(41\bar{5}0)$ plane of SiC has a simple potential. For channeled electrons of 300 MeV energy, two bound transverse states exist, and, therefore, channeling has a quantum character. An intense CR line can be observed from the one possible transition (Figs. 16 and 18). The energy of the 1→0 transition amounts to 1 MeV. At a depth of about 10 μm, statistical equilibrium for the occupation of states is reached (Fig. 17). This value is much bigger than those for the other planes. Therefore, it may be most suitable to use it as an intense quasi-monochromatic hard X-ray source for some CR application. For the electron energy of 800 MeV, four states are bound (Fig. 20) and channeling still can be described by quantum mechanics. The CR photon energies are shifted to higher energies, and due to the broader linewidths, the three CR lines cannot be resolved but may be superimposed forming a broad CR peak (Fig. 22). For the $(21\bar{3}0)$ and $(41\bar{5}0)$ planes at electron energies of order of several hundred MeV the number of bound states are relatively small, and, therefore, the quantum mechanical approach for the description of CR proves to be necessary. In Figs. 19 and 23 the spectral angular distribution of CR for electrons of energy 300 MeV and 800 MeV, which are simulated within classical approach have been presented.

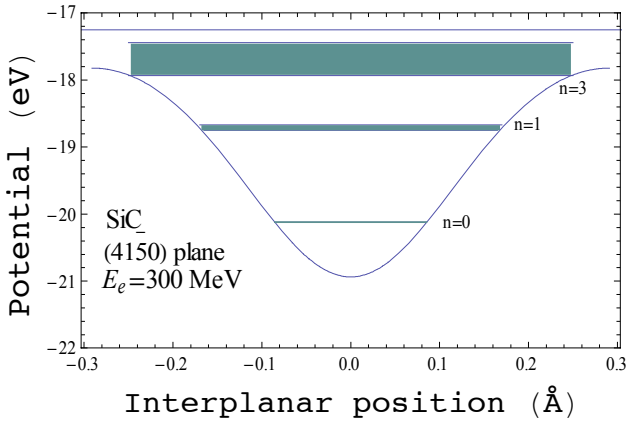

FIG. 16 – The $(41\bar{5}0)$ continuum potential and eigenvalues for 300 MeV electrons.

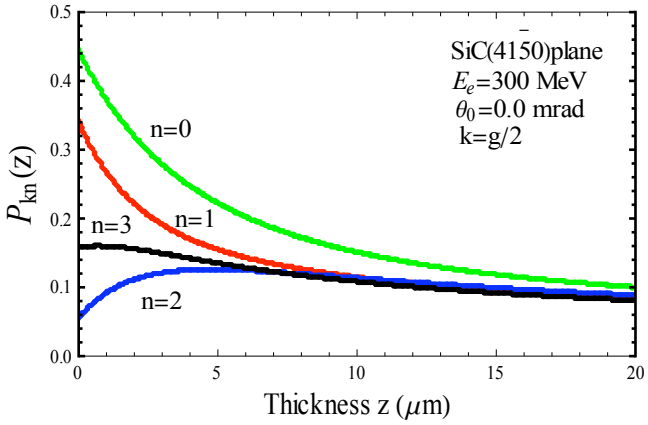

Fig. 17 - Depth dependence for the occupation of states versus the crystal thickness for 300 MeV electrons at 0.07 mrad incidence angle.

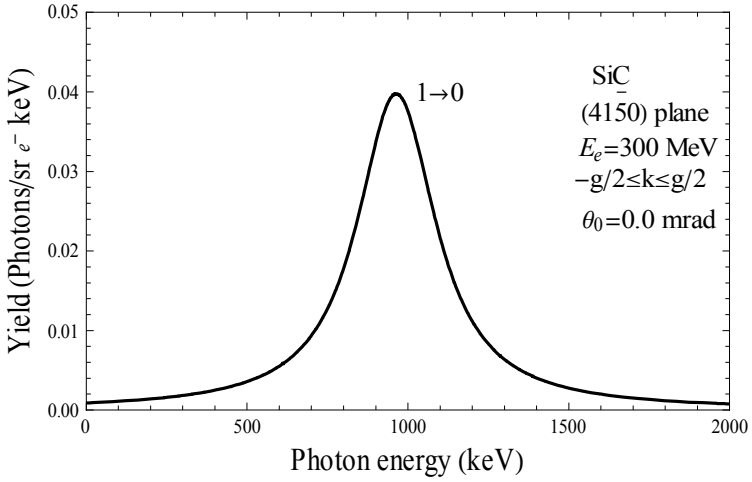

FIG. 18 – Quantum simulation of the CR spectrum for channeling of 300 MeV electrons in the $(41\bar{5}0)$ plane of a 20 μm thick SiC crystal.

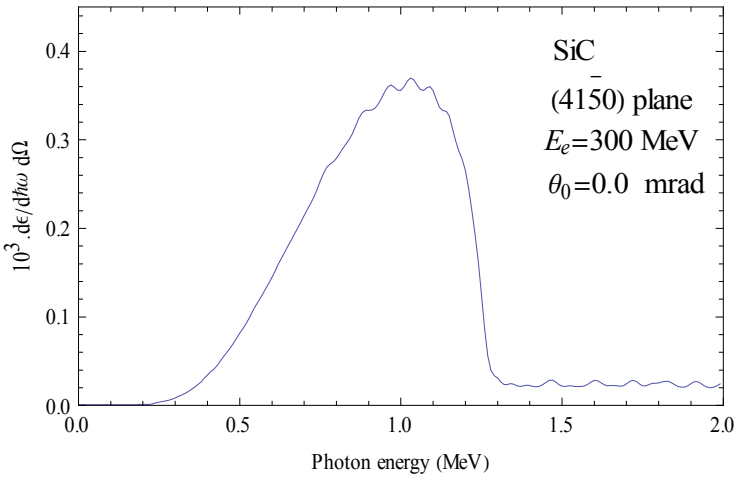

FIG. 19 – Classical simulation of the CR spectrum for channeling of 300 MeV electrons in the $(41\bar{5}0)$ plane of a 20 μm thick SiC crystal.

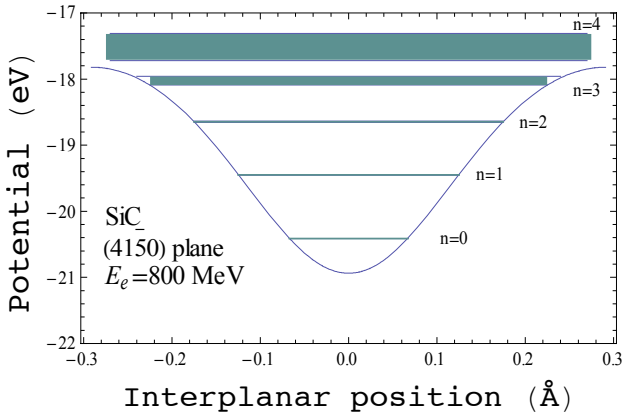

FIG. 20 – The $(41\bar{5}0)$ continuum potential and eigenvalues for 800 MeV electrons.

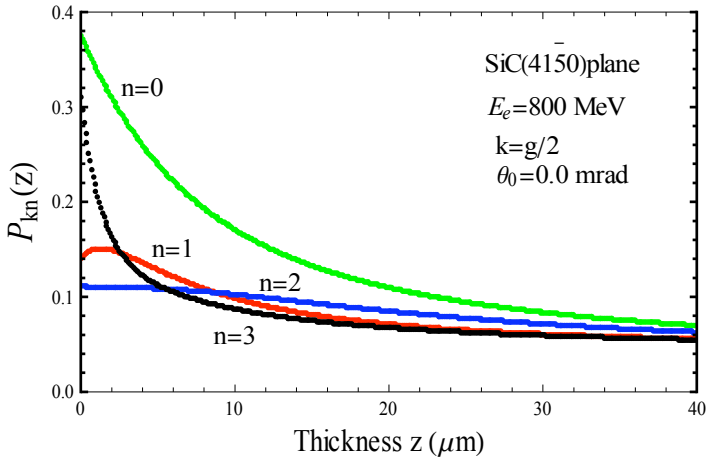

FIG. 21 – Depth dependence of the occupation of states drawn versus the crystal thickness for 800 MeV electrons at 0.03 mrad incidence angle.

FIG. 22 – Quantum simulation of the CR spectrum for channeling of 800 MeV electrons in the $(41\bar{5}0)$ plane of a 20 μm thick SiC crystal.

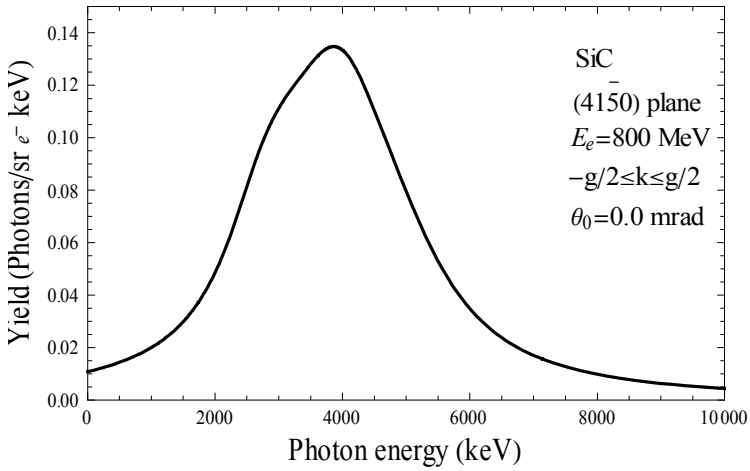

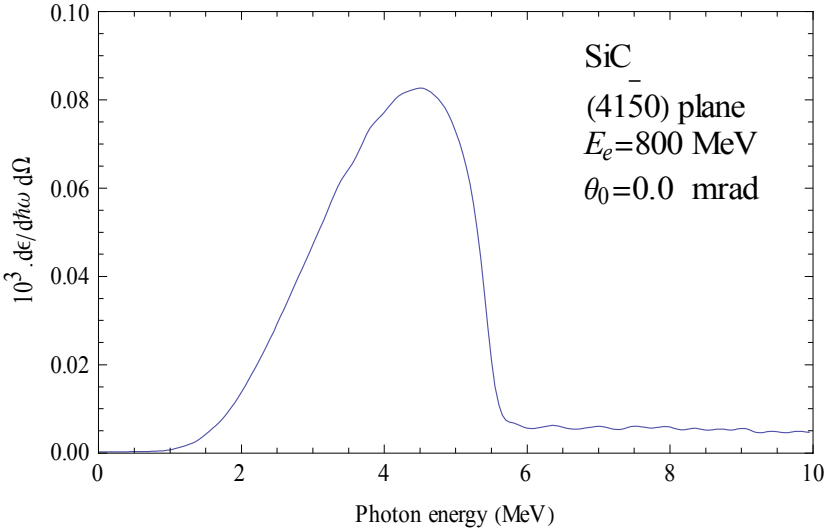

FIG. 23 – Classical simulation of the CR spectrum for channeling of 800 MeV electrons in the (41$\bar{5}$0) plane of a 20 μm thick SiC crystal.

In order to compare spectral line characteristics of CR for different planes, the transition energy, linewidth and intensity of the 1-0 transition and the total radiated intensity of all bound states at electron energy of 300 MeV for different planes are listed in Table 1. It should be underlined that the line intensities are calculated at zero thickness. It seems that in the case of the (11$\bar{2}$0) plane we can get the highest intensity, while the effective thickness for photon production is longer in (41$\bar{5}$0) plane.

TABLE 1. Calculated transition energy, linewidth and intensity of 1-0 transition together with total radiated intensity for planar channeling in SiC at electron energy of 300 MeV.

Plane	$E_{1\to0}$ *(MeV)*	$\Gamma_{\text{in } 1\to0}$ *(MeV)*	$\left[\frac{d^2N_{1\to0}}{d\Omega dz}\right]$ $\left[(photons/e)(sr\mu m)^{-1}\right]$	$\left[\frac{d^2N_{total}}{d\Omega dz}\right]$ $\left[(photons/e)(sr)^{-1}\right]$
(11$\bar{2}$0)	2.013	0.840	50.11	330.86
(21$\bar{3}$0)	0.665	0.126	14.03	22.32
(41$\bar{5}$0)	1.003	0.295	35.49	35.49

4. CONCLUSIONS

The hexagonal structure of 4H SiC provides a variety of planes with large difference in interplanar distances and depths of continuum potentials. Therefore, CR in

SiC crystals may have some specific features. It belongs to the space group $P6_3m$ and CR from planes with Miller indices l=0 that can be observed.

The CR spectrum have been simulated for the $(11\bar{2}0)$, $(21\bar{3}0)$ and the $(41\bar{5}0)$ planes of SiC crystal at different electron energies. The $(11\bar{2}0)$ plane has a simple and deep potential. Its depth is about 25 eV and its interplanar distance is 1.54 Å. For 20 MeV-electrons there are four bound states lead to 3 transitions, which are resolved in the spectrum. At electron moderate energies the number of bound states is large and channeling can be described within the frame of classical mechanics. This fact leads to unstructured "humps" shape. The $(11\bar{2}0)$ and $(41\bar{5}0)$ SiC planes are also characterized by a simple potential with the well depth of about 3 eV and the interplanar distance of 0.582 Å. At 300 MeV electron energy, the only two states with n=0 and n=1 are bound, and one CR line from corresponding transition $1\rightarrow0$ will be observed. 800 MeV electrons can populate three well separated transverse states in the $(41\bar{5}0)$ plane and produce a broad CR peak corresponding to two main transitions. The initial population of the states in the $(11\bar{2}0)$ plane is considerably smaller than that of the states in the $(41\bar{5}0)$ plane. Therefore, the $(41\bar{5}0)$ plane should be suitable to be used for some application of CR as an intense monochromatic X-ray source.

REFERENCES

1. M. Gouanere, D. Sillou, M. Spighel, N. Cue, M.J. Gaillard, R.G. Kirsch, J.-C. Poizat, J. Remillieux, B.L. Berman, P. Catillon, L. Roussel, and G.M. Temmer, *Nucl. Instr. Meth.* **194**, 225 (1982).
2. I. Reiz, Diploma thesis, TU Darmstadt (1999); H. Genz, in *Proc. NATO Advanced Research Workshop on Electron-Photon Interaction in Dense Media, Nor-Hamberd, Yerevan, Armenia (2001*) H. Wiedemann, Ed., NATO Science Series II, **49**, 217 (Kluwer Acad. Publ., Dordrecht, 2002).
3. B.Azadegan, W. Wagner, and J. Pawelke, *Phys. Rev.* **B74**, 045209 (2006).
4. M. Gouanere, D. Sillou, M. Spighel, N. Cue, M.J. Gaillard, R.G. Kirsch, J.-C. Poizat, J. Remillieux, B.L. Berman, P. Catillon, L. Roussel, and G.M. Temmer, *Phys. Rev.* **B38**, 4352 (1988).
5. J.U. Andersen, and E. Lægsgaard, *Phys. Rev. Lett.* **44**, 1079 (1980).
6. J.O. Kephart, B.L. Berman, R.H. Pantell, S. Datz, R.K. Klein, and H. Park, *Phys. Rev.* **B44**, 1992 (1991).

7. H. Park, R.L. Swent, J.O. Kephart, R.H. Pantell, B.L. Berman, S. Datz, and R.W. Fearick, *Phys. Lett.* **96A**, 45 (1983).
8. K. Chouffani, H. Überall, H. Genz, P. Hoffmann-Staschek, U. Nething, and A. Richter, *Nucl. Instr. Meth*. **B152**, 479 (1999).
9. J.U. Andersen, E. Bonderup, E. Lægsgaard, and A.H. Sørensen, *Phys. Scr.* **28**, 308 (1983).
10. C.K. Gary, A.S. Fisher, R.H. Pantell, J. Harris, and M.A. Piestrup, *Phys. Rev*. **B42**, 7 (1990).
11. G. Buschhorn, E. Dietrich, W. Kufner, M. Rzepka, H. Genz, H.-D. Gräf, P. Hoffmann-Staschek, U. Nething, and A. Richter, *Phys. Rev*. **B55**, 6196 (1997).
12. C.K. Gary, R.H. Pantell, M. Özcan, M.A. Piestrup, and D.G. Boyers, *J. Appl. Phys*. **70**, 2995 (1991).
13. B.L. Berman, S. Datz, R.W. Fearick, J.O. Kephart, R.H. Pantell, H. Park, and R.L. Swent, *Phys. Rev. Lett*. **49**, 474 (1982).
14. R.L. Swent, R.H. Pantell, H. Park, J.O. Kephart, R.K. Klein, S. Datz, R.W. Fearick, and B.L. Berman, *Phys. Rev*. **B29**, 52 (1984).
15. J. Freudenberger, H. Genz, L. Groening, P. Hoffmann-Staschek, W. Knüpfer, V.L. Morokhovskii, V.V. Morokhovskii, U. Nething, A. Richter, and J.P.F. Sellschop, *Nucl. Instr. Meth.* **B119**, 123 (1996).
16. W. Wagner, B. Azadegan, L.Sh. Grigoryan, and J. Pawelke, *Europhys. Lett.* **78**, 56004 (2007).
17. B. Azadegan, L.Sh. Grigoryan, J. Pawelke, and W. Wagner, *J. Phys. B: At. Mol. Opt. Phys.* **41**, 235101 (2008).
18. M.A. Kumakhov, and R. Wedell, *Radiation of Relativistic Light Particles during Interaction with Single Crystals* (Spektrum Akademischer Verlag, Heidelberg, 1991).
19. J. Lindhard, *Kong. Danske Vid. Selsk. Mat. Fys. Medd*. **14**, 34 (1965).
20. O. V. Bogdanov, K. B. Korotchenko, Yu. L. Pivovarov, and T. A. Tukhfatullin, *Nucl.Instr. Meth*. **B266**, 3858 (2008).
21. P.A. Doyle, and P.S. Turner, *Acta Crystallogr. Sect. A: Cryst. Phys. Diffr. Theor. Gen. Crystallogr.* **24**, 390 (1968).
22. N. Bernstein, H.J. Gotsis, D.A. Papaconstantopoulos, and M.J. Mehl, *Phys. Rev.* **B71**, 075203 (2005).